J Incl Phenom Macrocycl Chem (2009) 63:335–345
DOI 10.1007/s10847-008-9527-0

ORIGINAL ARTICLE

Fluorimetric study on the charge transfer behavior of *trans*-ethyl-(*p*-dimethylamino cinnamate) and its derivative in cyclodextrin cavities

T. Sanjoy Singh · Sivaprasad Mitra

Received: 16 August 2008 / Accepted: 10 December 2008 / Published online: 10 January 2009
© Springer Science+Business Media B.V. 2009

Abstract The intramolecular charge transfer (ICT) property of *trans*-ethyl *p*-(dimethylamino) cinnamate (EDAC) and its acid derivative, *p*-(dimethylamino) cinnamic acid (DMACA), is used to monitor the encapsulation behavior of these probes into the cyclodextrin (CD) nanocavities by steady state and picosecond time-resolved fluorescence spectroscopy. The ICT fluorescence band intensity was found to increase with concomitant blue shift in presence of cyclodextrins. The encapsulation behavior was further characterized by increase in emission yield, fluorescence anisotropy as well as lifetime values. Detailed analysis of the spectroscopic data indicate that the probes enter through the dimethyl amino group pointing to the secondary rim of the doughnut-shaped hydrophobic cavities to form 1:1 complex at different pH, however, the extent of penetration is more for EDAC compared with DMACA.

Keywords Intramolecular charge transfer (ICT) fluorescence · Cyclodextrin · Hydrophobic effect · Fluorescence lifetime and anisotropy · Binding constant

Introduction

Cyclodextrins are cyclic compounds containing six to eight glucose units, popularly known as α-, β-, or γ-cyclodextrin, respectively. They are known to form inclusion complexes with various low-molecular weight compounds, ranging from nonpolar aliphatic molecules to polar amines and acids [1]. Recently, much attention has been devoted to cyclodextrins as cyclic component for the construction of supramolecular architecture because of their well-defined ring structure and affinity for different class of compounds with varying size and shape. Although, cyclodextrins are known to form inclusion complexes with large compounds like metallocenes or polymers in different mechanisms [2, 3], a large variety of organic molecules act as host to form stable molecular assemblies inside the cyclodextrin nanocavities due to so called "hydrophobic effect" [4]. The unique property of cyclodextrins to encapsulate organic compounds inside its hydrophobic central cavity make them potential candidate as extremely efficient molecular vehicles for drug delivery. Furthermore, the reduced polarity and restricted geometry of the interior cyclodextrin cavities give an opportunity to study different photophysical properties in tailored environmental conditions.

Intramolecular charge transfer (ICT) process in electron donor–acceptor systems seems to be extremely important phenomenon in chemistry and biology. In the most widely studied ICT probe dimethyl amino benzonitrile (DMABN) and its derivatives, twisting of the donor dimethyl amino group with respect to the molecular plane in the excited state is thought to be associated with a large charge transfer from donor to acceptor causing an extra twisted intramolecular charge transfer (TICT) emission band in more polar environment [5]. However, reports from Zachariasse et al. argue for a different mechanism on the origin of the CT state and predicts that planarization of the dimethylamino group is far more active than twisting motion (PICT model) [6]. Nevertheless, the extreme sensitivity of these CT probes to polarity prompted a large number of studies of this process in a variety of cyclodextrin cavity [7–12].

In a recent study it was found that the ICT probe *trans*-ethyl *p*-(dimethylamino) cinnamate (EDAC, Scheme 1 for

T. S. Singh · S. Mitra (✉)
Department of Chemistry, North–Eastern Hill University, NEHU Permanent Campus, Umshing, Shillong 793 022, India
e-mail: sivaprasadm@yahoo.com; smitra@nehu.ac.in

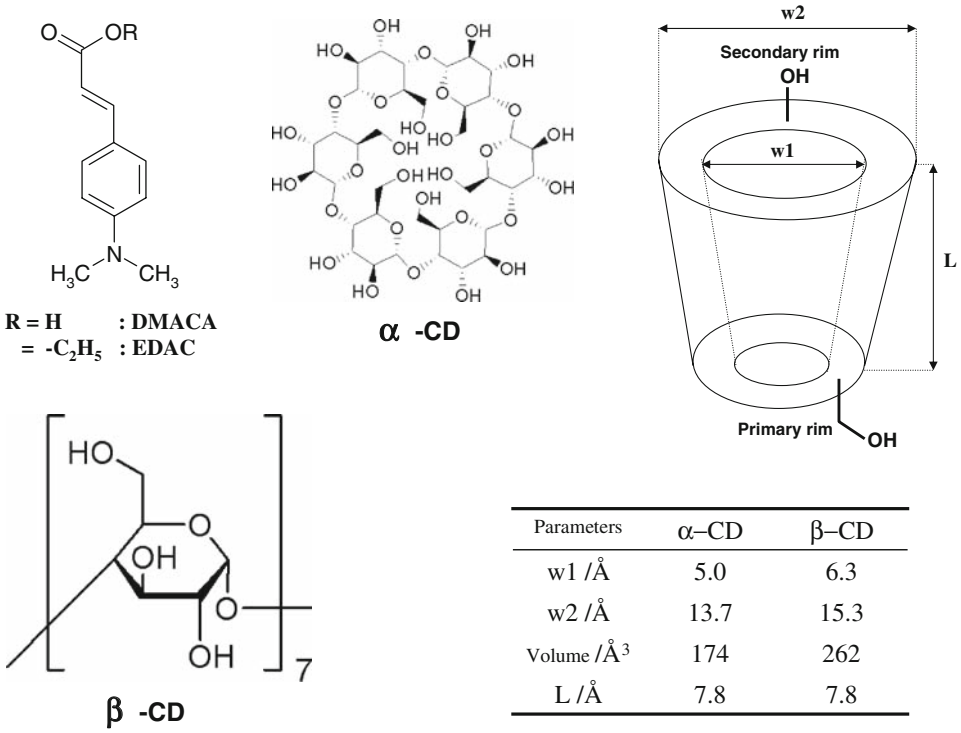

Scheme 1 Schematic diagram of the ICT probes EDAC and DMACA. The Chemical structures of both α- and β-CD are also shown along with the respective parameters for the host cavity

Parameters	α–CD	β–CD
w1 /Å	5.0	6.3
w2 /Å	13.7	15.3
Volume /Å^3	174	262
L /Å	7.8	7.8

structure) is extremely sensitive to solvent polarity and that the fluorescence properties show very good correlation with solvent polarity parameter [13]. The characterization of locally excited (LE) and ICT states was done and the change in dipole moment in the ground and excited states were calculated from steady state spectral measurements in a series of solvents with varying polarity using Lippert–Mataga relation [14]. The large change in ICT fluorescence spectra with solvent polarity prompts us to use EDAC as a probe to study the encapsulation in α- and β-CD cavities. The effect of pH on EDAC–CD complexation and the difference in binding properties of EDAC in α- and β-CD as host was compared with the complexation of a similar ICT probe 4-dimethylamino cinnamic acid (DMACA).

Experimental

(*trans*)-Ethyl *p*-(dimethylamino) cinnamate (EDAC) was synthesized using standard procedure based on Reformatsky reaction [15]. The crude compound was purified by column chromatography and repeated crystallization. Further characterization was done by NMR and infra-red spectroscopy. 4-(dimethylamino)-cinnamic acid (DMACA, 99%) was received from Alfa Aeser. The sample was further purified by repeated crystallization. α- and β-CD were all obtained from Aldrich Chemical Co. and used as received. The water used as solvent in all the measurements was obtained from Elix10 water purification system (Millipore India Pvt. Ltd.). All experimental solutions of varying pH were made with buffer (Qualigen). The chromophore concentration was very low (ca. 10 ∼ 12 μM) to avoid any aggregation, particularly for DMACA, and kept constant during the variation of cyclodextrin concentrations.

Steady state absorption spectra were recorded on a Perkin–Elmer model Lambda25 absorption spectrophotometer. Fluorescence spectra were taken in a Hitachi model FL4500 spectrofluorimeter and all the spectra were corrected for the instrument response function. Fluorescence quantum yields (ϕ_f) were calculated by comparing the total fluorescence intensity under the whole fluorescence spectral range with that of a standard (quinine sulfate in 1 M sulfuric acid) as described before [14].

Time-resolved fluorescence decay properties of the cyclodextrin encapsulated fluorophores were measured by picosecond time correlated single photon counting (TCSPC) technique. Except for the anisotropy measurements, all the fluorescence decays were collected at magic angle (54.7°) with respect to the vertically polarized excitation light, to avoid the effect of rotational depolarization of the probes on the measured fluorescence decay times. For EDAC, a picosecond diode laser (NanoLed-07, 408 nm) was used as the excitation source and a MCP-PMT based detection module as incorporated in the IBH instrument was used for measurement of fluorescence decays. The instrument response function for this setup is ∼100 ps (FWHM) [16]. On the other hand, a CW Nd:Vanadate (Vanguard, Spectra Physics, USA) pumped

rhodamine 6G dye laser with doubled tunable output was used for exciting the sample at 309 nm for DMACA [17]. The fluorescence emission was collected in a single photon counting mode with a MCP-PMT (R2809, Hamamatsu). The instrument response function (IRF, FWHM ~40 ps) was calculated using a dilute scattering solution of a diary creamer and by collecting the emission at the excitation wavelength.

The experimentally obtained fluorescence decay traces, I(t), were analyzed by non-linear least-square iterative convolution method based on Lavenberg–Marquardt algorithm and expressed as a sum of exponentials with Eq. 1

$$I(t) = \sum_i \alpha_i \exp(-t/\tau_i) \quad (1)$$

where, α_i is the amplitude of the i^{th} component associated with fluorescence lifetime τ_i such that $\sum \alpha_i = 1$.

The time-resolved fluorescence anisotropy decay curves were obtained by measuring the fluorescence emission intensity at parallel (I_{par}) and perpendicular (I_{per}) directions to the polarization of the excitation beam and constructing the time dependent anisotropy, r(t), with the following equation:

$$r(t) = \frac{I_{par}(t) - G(\lambda) I_{per}(t)}{I_{par}(t) + 2G(\lambda) I_{per}(t)} \quad (2)$$

where, G(λ) is the geometry factor at the wavelength λ of emission. The magnitude of geometry factor for the emission collection optics was determined independently as described elsewhere [16, 17].

Time-resolved anisotropy decays were analyzed with the following sets of equations:

$$I_{par}(t) = \frac{1}{3} I(t)[1 + 2r(t)] \quad (3)$$

$$I_{per}(t) = \frac{1}{3} I(t)[1 - r(t)] \quad (4)$$

$$r(t) = r_0 \sum \beta_j \exp(-t/\Theta_j) \quad (5)$$

where, r_0 is the initial anisotropy, β_j is the amplitude of the j^{th} correlation time (Θ_j) such that $\sum \beta_j = 1$.

Results and discussion

Photophysical properties of EDAC in aqueous medium: effect of pH

The absorption spectrum of EDAC in aqueous solution shows a broad and unstructured low-energy band with the maximum centered at around 365 nm. The room temperature fluorescence spectrum, originated from the intramolecular charge transfer (ICT) state, presents a maximum at 485 nm [14].

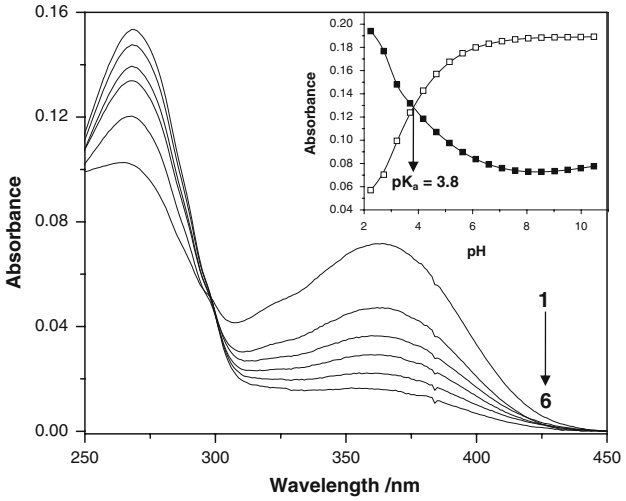

Fig. 1 Absorption spectra of EDAC (1.2×10^{-5} mol dm^{-3}) at pH 3.40 (1), 3.02 (2), 2.83 (3), 2.69 (4), 2.48 (5) and 2.24 (6). Inset shows the change in absorption intensity with solution pH at 360 nm (filled square) and 270 nm (empty square), respectively

The absorption and fluorescence properties of EDAC show drastic changes in presence of added acid. With decrease in pH of the solution, the absorption intensity of 365 nm band decreases with a concomitant increase of a new absorption band at 270 nm. An isosbestic point was observed at around 299 nm (Fig. 1). On the other hand, the intensity of fluorescence emission at 485 nm from the ICT state, obtained by excitation at 365 nm, decreases continuously with increase in acid concentration (Fig. 2). However, excitation at 270 nm, gives a new emission peak at 342 nm along with relatively weak emission at 485 nm, as shown in inset of Fig. 2. In presence of added acid, protonation occurs at the donor dimethyl amino group of EDAC and the following equilibrium is established with the protonated form ($EDACH^+$).

$$EDACH^+ \overset{pK_a}{\leftrightarrow} EDAC + H^+ \quad (6)$$

From the pH dependent spectrophotometric titration (inset, Fig. 1), the ground state pK_a value of $EDACH^+$ has been estimated to be 3.81 ± 0.05. It is to be noted here that, protonation on the dimethylamino group eliminates the possibility of intramolecular charge transfer upon excitation. So, the new absorption and emission band on the blue side in presence of added acid can be assigned as originated from the protonated structure of EDAC. This assignment was further confirmed by comparing the absorption (λ_{max} ~ 298 nm) and emission spectra (λ_{max} ~ 347 nm) of a model compound, *trans*-ethyl 4-nitro cinnamate (ENC), where ICT is not possible due to the presence of a nitro group in conjugation with the acceptor moiety.

The difference in pK_a values of the ground and excited state can be estimated from the steady state absorption (ν_a)

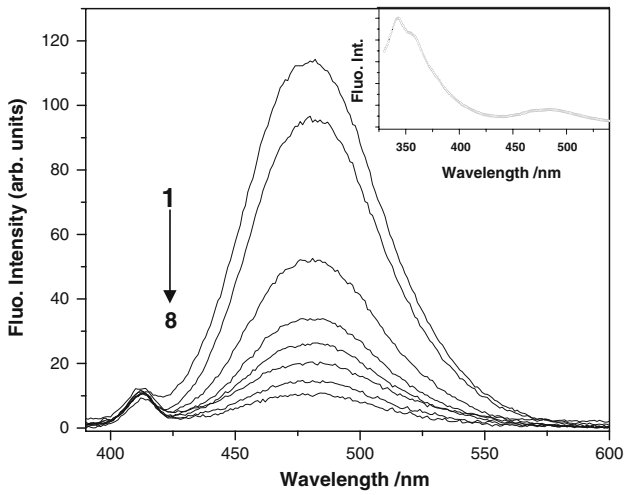

Fig. 2 Decrease in ICT fluorescence ($\lambda_{exc} = 365$ nm) emission intensity of EDAC (1.2×10^{-5} mol dm^{-3}) with pH. The solution pH are 6.77 (1), 3.40 (2), 3.01 (3), 2.83 (4), 2.69 (5), 2.48 (6), 2.39 (7) and 2.24 (8), respectively. Inset shows the fluorescence emission obtained by 270 nm excitation at pH = 2.83

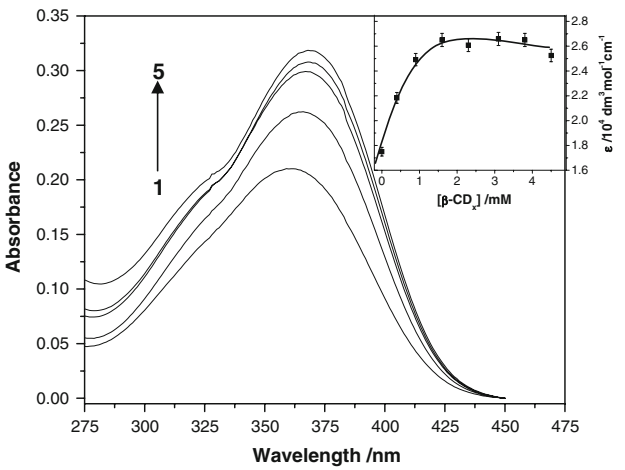

Fig. 3 Absorption spectra of EDAC (1.2×10^{-5} mol dm^{-3}) with increasing concentration of β-cyclodextrin at pH = 7.2. [β-CD]/mM are 1(0.0), 2(0.4), 3(0.9), 4(1.6) and 5(3.1). Inset shows the change in molar extinction coefficient

and fluorescence (v_f) maxima of the protonated (P) and deprotonated (D) form EDAC using the following equation [18]:

$$pK_a^* - pK_a = \frac{hc}{\kappa_B T \ln 10}\left(\frac{v_a^D + v_f^D}{2} - \frac{v_a^P + v_f^P}{2}\right) \quad (7)$$

The calculated value for EDAC is highly negative (approximately −18.9) which indicates very strong tendency of the protonated form to undergo deprotonation upon excitation. This explains the observation made in Fig. 2 (inset) that even on exciting the protonated form at 270 nm, the ICT band appears at 485 nm along with the fluorescence from the locally excited state of $EDACH^+$ at 342 nm.

Complexation in cyclodextrin nanocavities

Encapsulation of EDAC in cyclodextrin cavity: effect of pH

Complexation behavior of EDAC was monitored with both α- and β-cyclodextrins (CD) in buffer solutions of different pH. In presence of CD, it has been observed that absorption intensity increases with increase in the CD concentration in all the cases. A representative case of EDAC in β-CD is shown in Fig. 3. The value of molar extinction coefficient, shown in inset of Fig. 3, increases monotonically and then levels off beyond a certain range (∼2 mM) of CD concentration. The absorption peak position at 365 nm also shows bathochromic shift of about 8 ∼10 nm in CD environment. Both the increase in absorption intensity and shift in the peak maximum are indicative of penetration of the probe into the hydrophobic cavity toward the formation of a complex between the host and the probe molecule. The variation of 365 nm absorption peak with addition of CD is quite independent of solution pH. However, in acidic solution (pH ∼ 2.8), where the probe molecule mainly exists in the protonated form ($EDACH^+$), the 270 nm absorption shows hypsochromic shift of about 15 nm on addition of ∼11.5 mM of β-CD. Similar observation has been made for α-CD also.

As we have used the ICT emission to characterize the inclusion behavior of EDAC, the fluorescence emission only with 365 nm excitation was monitored. The fluorescence characteristics of EDAC in aqueous solutions at different pH are seen to undergo drastic changes in presence of cyclodextrins (Fig. 4). In all the cases, the fluorescence intensity increases with increase in CD concentration and then saturates to a limiting value beyond 4 ∼8 mM for α-CD and 1 ∼2 mM for β-CD. However, the concentration of CDs needed to reach this limiting value depends on pH of the solution (Fig. 5). In addition, the fluorescence spectra also show gradual blue shift on increasing concentration of CD. The absorption and fluorescence maxima for EDAC and its derivative in buffer solutions of different pH values are summarized in Table 1. For example, in presence of ∼5 mM β-CD, the fluorescence emission peak of EDAC ($\lambda_{max} = 465$ nm) shifts about 20 nm as compared to that observed in pure aqueous solution ($\lambda_{max} = 485$ nm). All these results also point towards the formation of EDAC–CD complex and correlates well with those observed in ground state absorption studies.

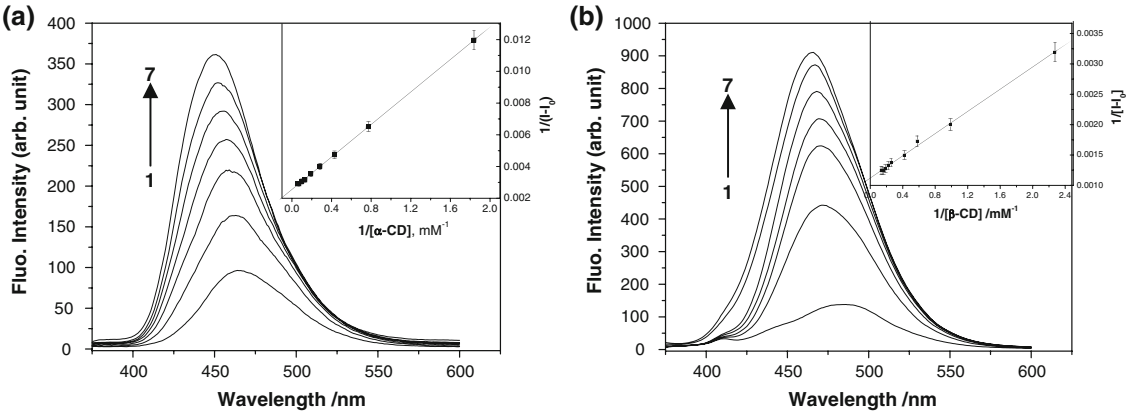

Fig. 4 Fluorescence emission spectra of EDAC (1.2×10^{-5} mol dm^{-3}) with increasing concentration of α-cyclodextrin at pH = 2.8 (**a**) and β-cyclodextrin at pH = 9.2 (**b**). The concentrations of CD (mM) are: (**a**) 0.5 (1), 1.29 (2), 2.32 (3), 3.53 (4), 5.24 (5), 7.5 (6), 17.62 (7) and (**b**) 0.0 (1), 0.44 (2), 1.02 (3), 1.74 (4), 2.38 (5), 4.51 (6), 5.3 (7). Inset shows the double reciprocal plot for 1:1 complex formation in the respective cases

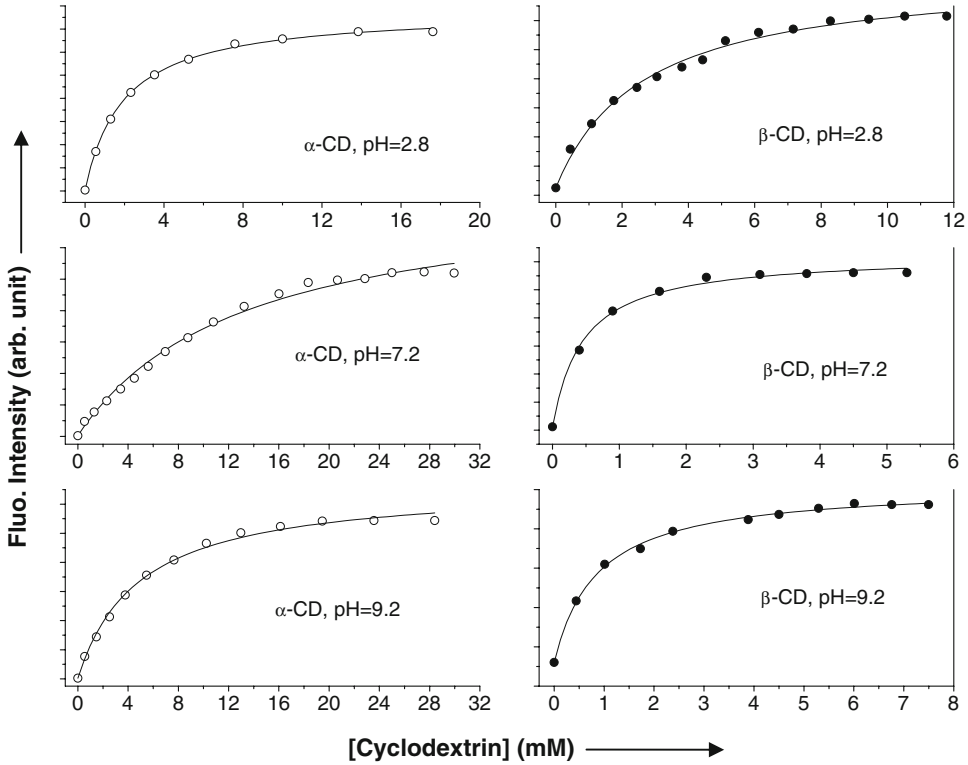

Fig. 5 Variation of EDAC fluorescence intensity against concentration of α-(open circle) and β-(filled circle) cyclodextrins at different pH. The solid lines indicate the non-linear fit to the experimental data using Eq. 14

Stoichiometry and association constant of host–guest complex

The stoichiometric ratio and apparent binding constant for EDAC/CD complex can be determined by analyzing the changes in ICT fluorescence emission with CD concentration. The equilibrium reaction for 1:1 binding between EDAC and CD can be written as

$$EDAC + CD \overset{K}{\leftrightarrow} EDAC : CD \tag{8}$$

The equilibrium constant for the above reaction is

$$K = \frac{[EDAC : CD]_{eq}}{[EDAC]_{eq}[CD]_{eq}} \tag{9}$$

If the initial concentration of the probe is represented by $[EDAC]_0$ and in the condition of $[CD] >> [EDAC]_0$, the above equation can be reduced to

$$K = \frac{[EDAC : CD]_{eq}}{([EDAC]_0 - [EDAC : CD]_{eq})[CD]} \tag{10}$$

At any instance, the observed fluorescence intensity (I) is the sum of the fluorescence intensities from the free and

Table 1 UV-visible absorption and fluorescence spectral properties of EDAC and DMACA in homogeneous buffer medium and on complexation with cyclodextrins

System	Medium pH	λ_{abs}/nm			λ_{em}/nm		
		Buffer	α-CD	β-CD	Buffer	α-CD	β-CD
EDAC	2.8	360	372	370	485	449	457
	7.2	360	370	368	484	447	467
	9.2	358	370	360	484	450	463
DMACA	2.8	357	365	367	476	449	466
	7.2	322	356	332	454	449	447
	9.2	300	292	300	456	444	446

Table 2 Binding constant, K (M^{-1}) of 1:1 complex of EDAC and DMACA with α- and β-cyclodextrin at different pH obtained by NLR method

pH	EDAC		DMACA	
	α-CD	β-CD	α-CD	β-CD
2.8	498 (22)	579 (28)	112 (15)	503 (30)
7.2	177 (15)	1,970 (59)	94 (15)	1,156 (48)
9.2	246 (20)	1,224 (47)	288 (19)	1,383 (50)

The absolute error in the calculation of K in each case are given in the parenthesis

bound EDAC, respectively. Under this condition, one can write

$$I = I_0 \frac{[EDAC]_{eq}}{[EDAC]_0} + I_\alpha \frac{[EDAC : CD]_{eq}}{[EDAC]_0} \tag{11}$$

where, I_0 and I_α are the fluorescence intensities of the *free* and *fully complexed* EDAC, respectively. Since, $[EDAC] = [EDAC]_{eq} + [EDAC : CD]_{eq}$, from Eq. 11 we can further write

$$\frac{[EDAC : CD]_{eq}}{[EDAC]_0} = \frac{I - I_0}{I_\alpha - I_0} \tag{12}$$

From Eqs. 10 and 12, the modified form of Benesi–Hilderbrand (BH) relation [19] can be written as

$$\frac{1}{I - I_0} = \frac{1}{I_\alpha - I_0} + \frac{1}{K(I_\alpha - I_0)} \times \frac{1}{[CD]} \tag{13}$$

Therefore, for an 1:1 complex formation, the double reciprocal plot of $1/(I-I_0)$ against 1/[CD] should give a straight line; from the slope and intercept of which, the equilibrium constant (K) can be calculated. Figure 4 (inset) shows some of the representative linear fitting using Eq. 13 and confirms that EDAC form 1:1 complex with both α- and β-cyclodextrin in varying experimental pH. The equilibrium constants can be calculated from the slope and intercept. The apparent K values obtained from the BH plot can be used as an initial guess in a non-linear regression (NLR) analysis to fit the fluorescence data directly using the following equation [20]

$$I = \frac{I_0 + I_1 K[CD]}{1 + K[CD]} \tag{14}$$

where, $I_1 = aI_0$, and a is the ratio of fluorescence quantum intensities of fully complexed and uncomplexed chromophore. The iterative NLR analysis based on Lavenberg–Marquardt algorithm was done using ORIGIN 6.0 (Microcal Inc.) software and the results are shown in Fig. 5 along with the K values mentioned in Table 2.

The increase in fluorescence quantum intensity of EDAC upon complexation with CD indicates the decrease in non-radiative decay process. Formation of the ICT state for DMABN type of molecules is known to be associated with an efficient low energy (~ 59 cm^{-1}) non-radiative decay mode for the motion of the dimethyl amino group [21]. Decrease in non-radiative process in CD environments, as observed from Table 3 and also discussed below, implies restricted motion of dimethylamino group. This indicates that EDAC penetrates the CD cavity efficiently pointing the dimethylamino group towards the core of the cavity. Figures 4 and 5 confirm the 1:1 complex formation of EDAC with both α- and β-cyclodextrin in different experimental pH. The K values given in Table 2 further reveal that complexation of EDAC in β-CD cavity is stronger than in α-CD. Although several literature results suggest 1:2 complex formation of the probe molecules like methyl 4-(dimethylamino) benzoate, 4′-dimethylamino-acetophenone and 2-methylnaphthalene, etc. with α-CD [22, 23], our experimental data do not provide any evidence for the formation of such a complex. Thus α-CD behaves similarly to β-CD, but its ability to encapsulate the probe is considerably smaller.

Extensive studies on molecular recognition by CDs have shown that the stabilities of the inclusion complexes are governed by simultaneous contribution of several weak forces such as hydrogen bonding, hydrophobic, dispersive and dipolar van der Waals interactions [24, 25]. All these forces are mainly determined by the size fit of the guest molecule into the CD cavity. Thus, since EDAC is approximately 5.1 Å in width [14], it should fit perfectly in β-CD, having cavity diameter of 6.0–6.5 Å [26]. On the other hand, the diameter of 4.7–5.3 Å in α-CD is not suitable for formation of proper host–guest complex due to very strong van der Waals interaction. This indicates that EDAC penetrates more toward the cyclodextrin cavity in the former than the later.

However, the K values are comparable at pH $\sim$2.8. As discussed in the previous section, at this experimental pH, EDAC remains mainly in the protonated state on the dimethylamino group. Penetration of charged dimethyl amino group is not favored inside the hydrophobic

Table 3 Summary of time-resolved decay parameters of EDAC and DMACA in cyclodextrin environment at different pH

System	Medium	pH	$\phi/10^{-3}$	Decay parameters						$<\tau>$/ns	$\kappa^r/10^6$ s^{-1}	$\sum\kappa^{nr}/10^9$ s^{-1}
				τ_1/ns	α_1%	τ_2/ns	α_2%	τ_3/ns	α_3%			
EDAC	Buffer	4.2	4.1	0.08	99	0.3	1	–	–	0.08	51.2	12.4
		7.2	3.4	0.08	99	0.4	1	–	–	0.09	37.7	11.0
		9.0	5.2	0.08	99	0.3	1	–	–	0.08	65.0	12.4
	α-CD	4.2	7.2	1.4	20	1.3	80	–	–	1.31	5.5	0.76
		7.2	19.3	1.2	11	1.4	89	–	–	1.35	14.3	0.73
		9.0	19.6	1.2	12	1.4	88	–	–	1.38	14.2	0.71
	β-CD	4.2	27.5	1.1	17	1.1	83	–	–	1.12	24.0	0.87
		7.2	9.5	0.04	25	1.1	75	–	–	1.13	8.4	0.88
		9.0	20.8	0.03	24	1.4	76	–	–	1.39	15.0	0.70
DMACA	Buffer	4.2	0.2	0.09	99	2.6	1	–	–	0.65	0.22	1.5
		7.2	0.8	0.03	40	0.09	60	–	–	0.08	9.7	12.6
		9.0	0.3	0.02	30	0.09	70	–	–	0.08	3.9	11.9
	α-CD	4.2	0.9	0.06	50	0.5	10	1.3	40	1.17	0.83	0.85
		7.2	1.4	0.13	30	0.4	50	1.1	20	0.72	1.9	1.39
		9.0	0.8	0.12	30	0.4	50	0.8	20	0.55	1.3	1.81
	β-CD	4.2	2.1	0.08	80	0.3	10	3.5	10	2.85	0.74	0.35
		7.2	9.9	0.08	60	0.2	30	0.4	10	0.22	45.0	4.58
		9.0	4.6	0.05	40	0.1	50	0.3	10	0.15	31.0	

nonpolar CD cavity. Consequently, under this condition, the binding process is not controlled by the size parameters of the hosts, and almost similar K value is observed for both α- and β-CD. However, relatively large difference in binding constant for the α- and β-CD, both at pH 7.2 and 9.2, indicates the suitability of the cavity size in the binding process with EDAC.

Comparison of EDAC encapsulation with 4-(dimethylamino)cinnamic acid (DMACA)

Photophysical properties and intramolecular charge transfer behavior of 4-(dimethylamino)cinnamic acid (DMACA) in different solvents were reported earlier in homogeneous solvents as well as in different heterogeneous medium [27, 28]. Some preliminary results on DMACA fluorescence in β-CD were reported [27]; however, no report of complexation with α-CD and pH dependence on DMACA–CD binding is available. Furthermore, no fluorescence data was used to evaluate the binding parameters. In this section, we extend the details of binding of DMACA with α- and β-CD using ICT emission of DMACA and compare the binding properties with EDAC at different pH.

The steady state spectral behavior of DMACA in presence of CDs is almost similar to that like EDAC (Table 1). It was found that DMACA also forms 1:1 inclusion complexes with both α- and β-CD. Similar treatment on the spectral data results the calculation of association constants of DMACA:CD binding and the values are reported in Table 2. It is seen that, for DMACA complexation with β-CD, the K values increase with increasing pH of the medium, contrarily to EDAC, for which the variation is irregular as described in the preceding section. It was shown earlier that the pK_a values corresponding to the protonation and deprotonation of the basic and acid functionalities of DMACA are 6.2 and 9.3, respectively [28]. Therefore, the experiments at pH 2.8 corresponds to the binding of protonated DMACA (similar to $EDACH^+$ discussed in previous section), whereas, at pH ~ 9.2, there may be some interference from deprotonated DMACA binding with CDs. However, the most interesting point to note here is that at around physiological pH (~7.2), the binding of EDAC is about two times more than DMACA (Table 2).

Time-resolved fluorescence decay behavior of host–guest complex

Fluorescence decay time measurements of both EDAC and DMACA were carried out in cyclodextrin environments at different pH using time correlated single photon counting method. The decay parameters along with other fluorescence quantum yield values are mentioned in Table 3 and some of the representative decay profiles are shown in Fig. 6. Although the decay time of EDAC fluorescence in homogeneous buffer solution could not be determined precisely due to instrument limited fluorescence decay

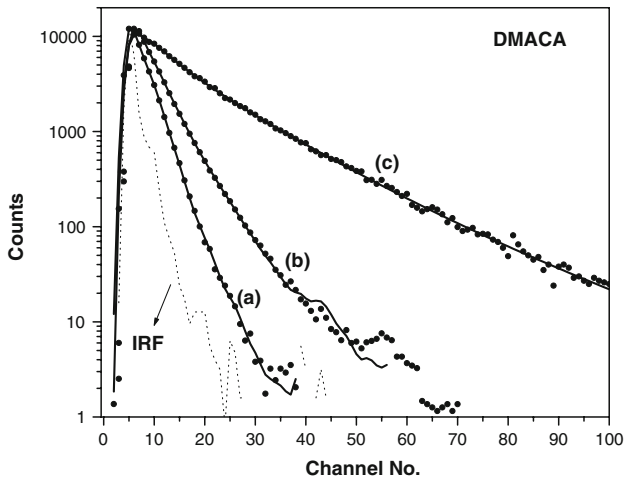

Fig. 6 Time resolved fluorescence decay traces (scattered points) alongwith the fitted data (solid line) of DMACA at pH 9.2 in homogeneous buffer (**a**), 5 mM β-CD (**b**), and 20 mM α-CD (**c**). The instrument response function (IRF) is also shown by dashed lines. Time increment is 42.8 ps/channel

behavior (see experimental section), the fluorescence due to charge transfer state of DMACA decays with a biexponential function. In general, the decay time increases substantially in presence of cyclodextrin while compared with the homogeneous solution. The same is true for DMACA also. The large increase in decay time in CD environment indicates a different microenvironment of the probes on encapsulation into the CD cavities.

Multiexponential decay of fluorescence in heterogeneous media is quite common and it is often difficult to mechanistically assign the various components of the decay [29]. Even if we assume that the diffusion of the probe molecule is rather slow in cyclodextrin environment, there is always a probability that a distribution of several host–guest complexes with different stoichiometry as well as varying degree of hydrophobicity are excited simultaneously to give multiexponential fluorescence decay. Instead of giving too much importance to individual decay components, we define the average decay time of the encapsulated fluorophore using Eq. 15 to discuss the fluorescence decay behavior [30].

$$<\tau> = \frac{\sum_i \alpha_i \times \tau_i^2}{\sum_i \alpha_i \times \tau_i} \qquad (15)$$

The calculated values are listed in Table 3. It is interesting to note that the mean fluorescence decay times ($<\tau>$ = 1.1–1.3 ns) of EDAC in cyclodextrin are about twelve to fifteen times more than in homogeneous solutions ($<\tau>$ = 0.09 ns) [14]. However, for DMACA the change is relatively less. For example, $<\tau>$ increases maximum by about six to nine times in presence of α-CD when compared with buffer solutions (Table 3). This difference further indicates that EDAC is encapsulated into the cyclodextrin cavity with much stronger interaction compared with that of DMACA as evidenced from the calculated association constant values mentioned in Table 2 and discussed earlier. Fluorescence quantum yield (ϕ) calculated from the area of the total fluorescence emission over the whole spectral range, the radiative (κ^r) and total non-radiative ($\sum\kappa^{nr}$) decay rate constants calculated from Eq. 16 are also listed in the same table. The increase in ϕ and substantial decrease in $\sum\kappa^{nr}$ in the CD environment points to the restricted motion of the fluorophore inside the cavities.

$$\kappa^r = \varphi/<\tau> ; \Sigma\kappa^{nr} = (1-\varphi)/<\tau> \qquad (16)$$

Structure of host–guest complex

Cyclodextrins (CDs), a family of torus-shaped cyclic oligosaccharides, are capable of forming inclusion complexes with organic molecules mostly through their secondary rims [31]. The size of α- and β-CD cavities (Scheme 1) are rather small with an inner and outer diameter ranging from 5.7 to 7.8 Å and 13.7 to 15.3 Å, respectively, whereas, the height is approximately 7.8 Å [26]. According to *ab-initio* calculation described earlier, the length and width of the probe EDAC is given by 12.2 and 5.2 Å, respectively [14]. This indicates that while the approach of EDAC towards β-CD cavity is favorable compared to α-CD, the environment around the probe inside the β-CD cavity is rather loose due to the availability of free space. Further, comparing the lengths, it can be said that a substantial portion of the probe will be projected out of the CD cavity.

To get an idea about the host-guest complexation behavior, time dependent fluorescence anisotropy decay were analyzed both in α- and β-CD environment. Figure 7 shows some of the representative anisotropy decay traces along with the simulated curve using Eq. 5 and Table 4 lists the rotational correlation time (Θ) for EDAC and DMACA in different environments. All the anisotropy decays could be fit satisfactorily with single exponential function. The anisotropy decay time of both EDAC and DMACA are of the order of several 100 ps (500–900 ps) in α-CD. However, surprisingly in β-CD, the anisotropy decay is very fast (100–150 ps) for EDAC whereas, for DMACA it is beyond the resolution of detection system. Although, at this point, the origin of very fast anisotropy decay in β-CD is not very clear, it can be assumed as due to the rapid segmental motion of probe inside the cavity. The possible interference through scattered light can be negated considering similar experimental condition for both α- and β-CD environment. Furthermore, the presence of free probe, which may also contribute towards faster anisotropy decay, can be ruled out in the case of β-CD considering the

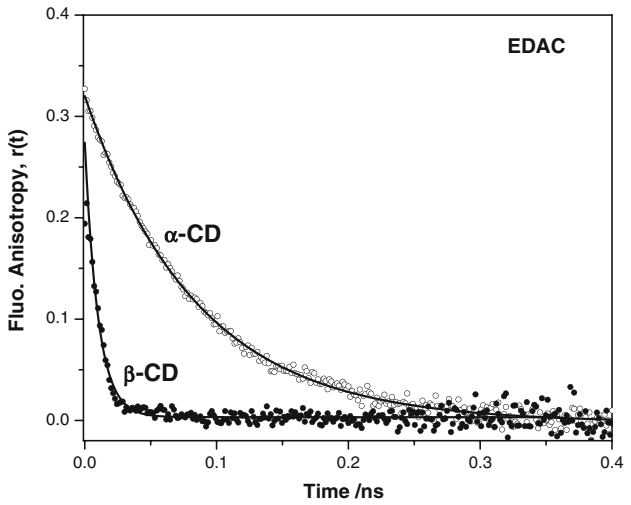

Fig. 7 Decay kinetics of fluorescence anisotropy of EDAC in α- and β-cyclodextrins ([CD] = 20 mM and 5 mM, respectively) at pH = 7.2

Table 4 Rotational correlation time (Θ) of EDAC and DMACA with α- and β-cyclodextrin at different pH obtained by time dependent fluorescence anisotropy measurement

System	Medium	pH	Θ/ps
EDAC	α-CD	4.2	880
		7.2	840
		9.0	890
	β-CD	4.2	140
		7.2	100
		9.0	130
DMACA	α-CD	4.2	800
		7.2	550
		9.0	475

Anisotropy decay for both the probes in homogeneous solutions as well as for DMACA in β-CD is instrument limited

higher binding constant of the host–guest complex compared with α-CD. The hydrodynamic diameter (d_{rot}) corresponding to rotational correlation time, Θ, can be calculated assuming a spherical volume (V) of the rotor

$$d_{rot} = \sqrt[3]{\frac{6V}{\pi}} \tag{17}$$

on the basis of Debye–Stokes–Einstein relation given by

$$\Theta = \frac{V\eta f C}{k_B T} \tag{18}$$

where, η is the viscosity of the medium, k_B is Boltzmann constant, T is temperature, f is a form factor set to 1 for spherical objects and C is a correction factor varying between 0 and 1 depending on sticking or slipping conditions [32, 33]. Using the measured viscosity of ~1.2 mPa s for 7.5 mM α-CD solution at 20°C and a correction factor of 0.4 from Gierer–Wirtz model, details of which was described earlier [34], d_{rot} was calculated to be 19 Å for EDAC.α-CD complex, which is almost equal to the sum of the height of α-CD and the length of the probe (7.8 and 12.2 Å, respectively). This indicates very little encapsulation of the probe inside the α-CD cavity and consistent with very small association constant described earlier. On the contrary, similar treatment of β-CD data leads to d_{rot} ~10 Å indicating almost full encapsulation of the probe inside β-CD cavity.

It would be interesting to get a clear picture of the binding mechanism of both EDAC and DMACA with CDs. More particularly, the approach of the probe towards the cyclodextrin cavity can be of two distinct type's viz. the incorporation of dimethylamino group towards or opposite to the secondary rim of cyclodextrin cavity. As discussed earlier, time-resolved studies on the host–guest complex point towards the projection of dimethylamino group into the CD cavity. Furthermore, approach through the carboxylate group in EDAC should experience more van der Waals interaction inside the cavity. On the other hand, the carboxylate group of EDAC, if projected outside the cavity, can form additional hydrogen bond with the hydroxyl group on the secondary rim of β-CD. Molecular modeling calculation can indeed help in understanding this incorporation and preliminary results for EDAC:β-CD system is in favor of the mechanism where dimethylamino group of the probe approaches through the secondary rim of the cyclodextrin cavity. More complete analysis of the results is in progress to understand the geometry of different inclusion modes of the guests as well as the relative contribution of several forces driving towards the host–guest complex formation, both in vacuum and also in aqueous medium.

Conclusion

Fluorescence properties of polarity sensitive charge transfer probe EDAC and its acid derivative DMACA were found to be modified in cyclodextrin medium when compared with aqueous bulk phase. The encapsulation and binding of the probes into the cyclodextrin nanocavities were monitored with shift in steady state absorption and fluorescence peak maximum as well as increase in mean fluorescence decay time. Both these probes form 1:1 inclusion complexes with β- as well as with α-cyclodextrin at different pH. However, the parameters like equilibrium constant and time-resolved fluorescence decay behavior point towards the more efficient complex formation in the former. Experimental results at different pH as well as fluorescence anisotropy measurements indicate the approach of the probe through the

dimethylamino group towards the secondary rim of the cyclodextrin cavity.

Acknowledgment Financial support from Council of Scientific & Industrial Research (CSIR) and Department of Science & Technology (DST), Government of India is gratefully acknowledged. The authors are indebted to Profs. G. Krishnamoorthy and H. Pal of TIFR and BARC, respectively, for their help in TCSPC measurements. Thanks are also due to University Grants commission (UGC) and DST for supporting the Department of Chemistry through DSA-SAP and FIST, respectively.

References

1. Szejtli, J.L.: Industrial application of cyclodextrin. In: Atwood, J.L., Davies, J.E.D., MacNicol, D.D., Vögtle, F. (eds.) Comprehensive Supramolecular Chemistry, vol. 3 . Elsevier, Oxford, UK (1996)
2. Odagaki, Y., Hirotsu, K., Higuchi, T., Harada, A., Takahashi, S.: X-Ray structure of the α-cyclodextrin–ferrocene (2:1) inclusion compound. J. Chem. Soc. Perkin Trans **1**, 1230–1231 (1990). doi:10.1039/p19900001230
3. Harada, A.: Synthesis of Polymers. In: Schlüter, A.-D. (ed.) Wiley – VCH, Weinheim (1999)
4. Kalyansundaram, K.: Photochemistry in microheterogeneous systems, p. 299. Academic Press, Orlando, FL (1987)
5. Grabowski, Z.R., Rotkiewicz, K.: Structural changes accompanying intramolecular electron transfer: Focus on twisted intramolecular charge-transfer states and structures. Chem. Rev **103**, 3899–4032 (2003). doi:10.1021/cr9407451
6. Zachariasse, K.A., Druzhinin, S.I., Bosch, W., Machinek, R.: Intramolecular charge transfer with the planarized 4-aminobenzonitrile 1-*tert*-butyl-6-cyano-1,2,3,4-tetrahydroquinoline (NTC6). J. Am. Chem. Soc **126**, 1705–1715 (2004). doi:10.1021/ja037544w
7. Kim, Y.H., Cho, D.W., Yoon, M., Kim, D.: Observation of hydrogen-bonding effects on twisted intramolecular charge transfer of *p*-(*N*,*N*-diethylamino)benzoic acid in aqueous cyclodextrin solutions. J. Phys. Chem **100**, 15670–15676 (1996). doi:10.1021/jp9613652
8. Das, S.K.: Inclusion complexation of 2-(4′-*N*,*N*-dimethylaminophenyl)-*1H*-naphth[*2,3-d*]imidazole by *β*-cyclodextrin: effect on the twisted intramolecular charge transfer emission. Chem. Phys. Lett **361**, 21–28 (2002). doi:10.1016/S0009-2614(02)00903-X
9. Hamai, S.: Effects of cyclodextrins on the fluorescence of 2-Methylnaphth[2,3-*d*]oxazole in aqueous solution. Bull. Chem. Soc. Jpn **77**, 1459–1464 (2004). doi:10.1246/bcsj.77.1459
10. Singh, M.K., Pal, H., Koti, A.S.R., Sapre, A.V.: Photophysical properties and rotational relaxation dynamics of neutral red bound to *β*-cyclodextrin. J. Phys. Chem. A **108**, 1465–1474 (2004). doi:10.1021/jp035075e
11. Park, J.W., Lee, S.Y., Kim, S.M.: Efficient inclusion complexation and intra-complex excitation energy transfer between aromatic group-modified *β*-cyclodextrins and a hemicyanine dye. J. Photochem. Photobiol. Chem **173**, 271–278 (2005)
12. Stalin, T., Rajendiran, N.: Intramolecular charge transfer effects on 3-aminobenzoic acid. Chem. Phys **322**, 311–322 (2006). doi:10.1016/j.chemphys.2005.09.002
13. Singh, T.S., Mitra, S.: Fluorescence behavior of intramolecular charge transfer probe in anionic, cationic, and nonionic micelles. J. Colloid Interface Sci **311**, 128–134 (2007). doi:10.1016/j.jcis.2007.02.046
14. Singh, T.S., Mitra, S., Chandra, A.K., Tamai, N., Kar, S.: A combined experimental and theoretical study on photoinduced intramolecular charge transfer in *trans*-ethyl *p*-(dimethylamino)cinnamate. J. Photochem. Photobiol. Chem **197**, 295–305 (2008). doi:10.1016/j.jphotochem.2008.01.007
15. Vogel, A.: Textbook of Practical Organic Chemistry, 4th edn, p. 535. ELBS, London (1978)
16. Dutta Choudhury, S., Kumbhakar, M., Nath, S., Pal, H.: Photoinduced bimolecular electron transfer kinetics in small unilamellar vesicles. J. Chem. Phys **127**, 194901–194913 (2007). doi:10.1063/1.2794765
17. Nag, N., Rao, B.J., Krishnamoorthy, G.: Altered dynamics of DNA bases to a mismatch: A cue for mismatch recognition by Muts. J. Mol. Biol **374**, 39–53 (2007). doi:10.1016/j.jmb.2007.08.065
18. Förster, Th.: Electrolytic dissociation of excited molecules. Z. Elecktrochem. **54**, 42–46 (1950)
19. Benesi, H.A., Hilderbrand, J.H.: A spectrophotometric investigation of the interaction of iodine with aromatic hydrocarbons. J. Am. Chem. Soc **71**, 2703–2707 (1949). doi:10.1021/ja01176a030
20. Mitra, S., Das, R., Mukherjee, S.: Intramolecular proton transfer in inclusion complexes of cyclodextrins: Role of water and highly polar nonaqueous media. J. Phys. Chem. B **102**, 3730–3735 (1998). doi:10.1021/jp972779d
21. Schamschule, R., Parusel, A., Köhler, G.: Theoretical investigations of the ground-state properties of stereoselectively substituted aminobenzonitriles. J. Mol. Struct. THEOCHEM **419**, 161–167 (1997). doi:10.1016/S0166-1280(97)00182-6
22. Matsushita, Y., Suzuki, T., Ichimura, T., Hikida, T.: Cavity size effect on the excited state dynamics of methyl 4-(dimethylamino)benzoate−cyclodextrin complexes. J. Phys. Chem. A **108**, 7490–7496 (2004). doi:10.1021/jp036624j
23. Hamai, S.: Inclusion behavior of α-cyclodextrin with 2-methylnaphthalene in aqueous solutions. J. Incl. Phenom. Macrocycl. Chem **27**, 57–67 (1997). doi:10.1023/A:1007955123149
24. Saenger, W.: Cyclodextrin inclusion compounds in research and industry. Angew. Chem. Int. Ed. Engl **19**, 344–362 (1980). doi:10.1002/anie.198003441
25. Connors, K.A.: The stability of cyclodextrin complexes in solution. Chem. Rev **97**, 1325–1358 (1997). doi:10.1021/cr960371r
26. Szejtli, J.: Introduction and general overview of cyclodextrin chemistry. Chem, J. Rev **98**, 1743–1754 (1998)
27. Bangal, P.R., Chakravorti, S.: Photophysics of 4-dimethylamino cinnamic acid in different environments. J. Photochem. Photobiol. Chem **116**, 191–202 (1998). doi:10.1016/S1010-6030(98)00303-7
28. Singh, T.S., Mitra, S.: Fluorimetric studies on the binding of 4-(dimethylamino)cinnamic acid with micelles and bovine serum albumin. Photochem. Photobiol. Sci **7**, 1063–1070 (2008). doi:10.1039/b717475f
29. Das, P., Mullick, A., Chakrabarty, A., Halder, B., Chattopadhyay, N.: Effect of nanocavity confinement on the rotational relaxation dynamics: 3-acetyl-4-oxo-6,7-dihydro-12*H* indolo-[2,3-*a*] quinolizine in micelles. J. Chem. Phys **125**, 44516–44521 (2006). doi:10.1063/1.2219751
30. Lackowicz, J.R.: Principles of fluorescence spectroscopy. Springer, Singapore (2006)
31. Banerjee, A., Sengupta, B., Chaudhuri, S., Basu, K., Sengupta, P.K.: Encapsulation of Prodan in beta-cyclodextrin environments: A critical study via electronic spectroscopy and molecular mechanics. J. Mol. Struct **794**, 181–189 (2006). doi:10.1016/j.molstruc.2006.02.012
32. Fleming, G.R.: Chemical Applications of Ultrafast Spectroscopy. Oxford University Press, London (1986)
33. Hu, M.C., Zwanzig, R.: Rotational friction coefficients for spheroids with the slipping boundary condition. J. Chem. Phys **60**, 4354–4357 (1974). doi:10.1063/1.1680910

34. Maus, M., De, R., Lor, M., Weil, T., Mitra, S., Wiesier, U.-M., Hermann, A., Hofkens, J., Vosch, T., Müllen, K., De Schryver, F.C.: Intramolecular energy hopping and energy trapping in polyphenylene dendrimers with multiple peryleneimide donor chromophores and a terryleneimide acceptor trap chromophore. J. Am. Chem. Soc **123**, 7668–7676 (2001). doi:10.1021/ja010570e